Original Article

JCBFM

Journal of Cerebral Blood Flow & Metabolism
2018, Vol. 38(10) 1769–1780

DOI: 10.1177/0271678X17715813
journals.sagepub.com/home/jcbfm
SAGE

Two-kidney one-clip is a pertinent approach to integrate arterial hypertension in animal models of stroke: Serial magnetic resonance imaging studies of brain lesions before and during cerebral ischemia

Benjamin Ménard, Laurent Chazalviel, Simon Roussel, Myriam Bernaudin and Omar Touzani

Abstract

Although chronic arterial hypertension (CAH) represents the major comorbid factor in stroke, it is rarely integrated in preclinical studies of stroke. The majority of those investigations employ spontaneously hypertensive rats (SHR) which display a susceptibility to ischemic damage independent of hypertension. Here, we used a renovascular model of hypertension (RH) to examine, with magnetic resonance imaging (MRI), brain alterations during the development of hypertension and after brain ischemia. We also examined whether MRI-derived parameters predict the extent of ischemia-induced brain damage. RH was induced according to the two-kidney one-clip model and multiparametric MRI was performed at 3, 6, 9, and 12 weeks after hypertension and also at 10, 50, and 60 min following stroke. Blood pressure values increased progressively and reached a plateau at 6 weeks after RH induction. At 12 weeks, all hypertensive animals displayed spontaneous brain lesions (hemorrhages, deep and cortical lesions, ventricular dilatation), increased apparent diffusion coefficient (ADC) values in the corpus callosum and higher fractional anisotropy in the cortex. Following ischemia, these animals showed larger brain lesions (406 ± 82 vs. $179 \pm 36\,mm^3$, $p < 0.002$) which correlated with ADC values at chronic stage of hypertension. This model of hypertension displays many characteristics of the neuropathology of human CAH. The use of this model in stroke studies is relevant and desirable.

Keywords

Stroke, hypertension, magnetic resonance imaging, Goldblatt, risk factor

Received 14 November 2016; Accepted 16 May 2017

Introduction

Stroke is currently the third leading cause of death and of major disabilities in the industrialized countries.[1] The only treatments currently approved by health authorities for stroke are thrombolysis with the tissue plasminogen activator or mechanical thrombectomy, which are administered only within the first hours after the initial onset of symptoms and can be applied solely to a minority of the patients that enter into this therapeutic window and present no radiologic signs of intracranial hemorrhage.[2]

Brain ischemia research now faces a major challenge because of the difficulty in translating the preclinical demonstration of neuroprotection into therapeutic benefit in human stroke.[3] One of the issues that has been put forward to explain this failure is the inadequacy of the animal models of stroke.[4–6] Most of the available preclinical studies rely on the use of young,

Normandie Univ, UNICAEN, CNRS, CEA, ISTCT/CERVOxy group, Caen, France

Corresponding author:
Omar Touzani, CERVOxy group, ISTCT Unit, GIP CYCERON, Bd Henri Becquerel, BP5229, 14074 CAEN Cedex, France.
Email: touzani@cyceron.fr

healthy animals devoid of concomitant, or underlying pathologies such as chronic arterial hypertension (CAH).[5,6]

CAH, a critical public health problem in the world and the major modifiable risk and aggravating factor for all subtypes of stroke,[7–9] is often ignored in experimental studies of ischemic stroke. Accordingly, many expert groups have forcefully recommended the integration of CAH in preclinical animal studies aimed to test a given therapeutic strategy for stroke.[10–12]

Therefore, the question now is how to integrate CAH into experimental stroke studies and what animal model of hypertension would be the most pertinent with respect to future clinical investigations. Many models of CAH have been reported, but the great majority of the experimental stroke studies have used spontaneously hypertensive rats (SHR) and their related strain, spontaneously hypertensive rats–stroke prone (SHR-SP).[5,13] However, these strains of rats are well known to display, in part, a genetic vulnerability to ischemia-induced brain lesions independent of the arterial hypertension.[14,15]

Based on these observations, an alternative and complementary model of hypertension ought to be employed to take this comorbidity into account in animal stroke studies. One of these models is the Goldblatt procedure which mimics renovascular hypertension, that accounts for 5–10% of hypertensive patients.[16–19] This model of hypertension would also be used broadly in the vascular-cognitive research field since hypertension and stroke are highly prevalent risk factors for cognitive impairment and dementia.[20]

In the rat, chronic renovascular hypertension, induced by stenosis of the renal artery, is known to induce structural and functional alterations in the cerebrovascular tree similar to those described in SHR.[21,22] Nonetheless, parenchymal alterations during the development of hypertension and after brain ischemia are less well characterized. In the present study, with conventional T2-weighted magnetic resonance imaging (T2-WI) and diffusion-weighted imaging (DWI), we analyzed firstly, hypertension-induced brain lesions and changes in the values of the apparent diffusion coefficient (ADC) and fractional anisotropy (FA), and secondly, examined whether these magnetic resonance imaging (MRI)-derived parameters could predict the extent of brain damage induced by transient focal cerebral ischemia. DWI-derived parameters are increasingly documented to be a correlate of microstructural changes in different neurological diseases[23,24] and therefore could provide noninvasive early markers of disease. In the context of CAH, identification of early cerebral changes associated with later development of stroke or dementia could be of importance in the management of hypertensive patients.

Materials and methods

Animals

Twenty male Sprague-Dawley rats, purchased from the R Janvier Breeding center, le Genest Saint-Isle, France, were included in the study. At the beginning of the protocol, all rats were 4 weeks old and were maintained in a temperature-controlled housing with 12 h day/night cycle with food and water ad libitum. The experimental procedure was approved by the Regional Ethic Committee for Animal Research (CENOMEXA N/21-11-06/21) and carried out in accordance with the EU Directive 2010/63/EU for animal experiments. Data are reported according to ARRIVE guidelines. All the experiments were performed randomly (a random draw was made for group allocation and for imaging examinations) and the data were analyzed in a blind manner. Based on the available literature and a power analysis, 20 animals were included in this study. Twelve rats were subjected to renovascular hypertension (HT group) and eight remained normotensive (NT group). Three rats of the HT group died after 6–9 weeks following the induction of hypertension (two developed severe brain hemorrhage and one was found dead in its cage, but the cause of death could not be determined). These rats were excluded from the analyses.

Induction of renovascular hypertension

Chronic renovascular arterial hypertension was induced according to the two-kidney one-clip model (2K-1C) in 4-week-old rats.[25] Briefly, rats were anesthetized with 2–3% isoflurane in N_2O/O_2:70%/30% and a paramedian laparotomy was performed to expose one renal artery. A U-shaped silver clip with an inner diameter of 200 µm was placed around the proximal segment of the artery to induce stenosis. Abdominal muscle and skin were sutured and the rats received an analgesic (Tolfedine® 4%, 4 mg/kg i.m) and saline (2 ml, i.p.) and thereafter recovered from anesthesia. Control sham was subjected to the same surgical procedure, but the clip was not placed on the renal artery.

Arterial pressure measurements

Systolic arterial pressure (sAP) was measured in awake rats by the tail cuff technique (BP-2000 Blood Pressure Analysis System™ Visitech Systems) as described by Letourneur and colleagues (2011).[25] sAP was measured before and at three weeks after the surgical procedure, and thereafter, every week during the nine remaining weeks of the protocol. During each measurement session, rats were prewarmed and subjected to 15 consecutive measurements of sAP. The first five measures were discarded.

Induction of cerebral ischemia

Twelve weeks following the induction of hypertension, the induction of anesthesia was achieved with isoflurane (5%), then the rats were intubated and artificially ventilated (MRI-1 Ventilator; CWE, Inc.). Anesthesia was subsequently maintained by inhalation of isoflurane (1.8–2.5%) in a mixture of N_2O/O_2: 70%/30%. End tidal CO_2 was continuously measured (Microcapnograph CI240 Columbus Instruments, Columbus, OH, USA) and corrected as necessary. The femoral artery was canulated for assessment of arterial pressure and gases. Rectal temperature was monitored and maintained around 37.5°C with a thermostatically controlled heating pad (Homeothermic Blanket, Harvard) throughout the anesthesia.

Brain ischemia was induced by 1 h temporary middle cerebral artery occlusion (MCAo) by the intraluminal approach.[25] Briefly, a nylon thread with a distal stump (3 mm in length and 380 µm in outer diameter) was inserted retrogradely into the external carotid artery and gently advanced to reach the origin of the MCA. Magnetic resonance (MR) angiography angiography was performed immediately after the occlusion and repeated following the reperfusion.

Magnetic resonance imaging

Each rat underwent a series of MRI examinations according to the protocol represented in Figure 1. MRI was performed on a Bruker Pharmascan 7-Tesla horizontal magnet. Rats were anesthetized by isoflurane (1.8% to 2.5%) in N_2O/O_2:70%/30% and placed in a stereotaxic head holder within the magnet. Physiological parameters were monitored in the MRI suite as described above.

A scout image was first performed (fast low angle shot sequence; repetition time (TR)/echo time (TE) = 100/4 ms; resolution 0.39 mm × 0.39 mm × 3 mm, acquisition time = 12.8 s) in order to control and adjust the position of animals within the magnet. Then, the following imaging examinations were performed: T2-WI sequences (Rapid Acquisition with Relaxation Enhancement (RARE) factor = 8, TR/TE = 5000/65 ms; number of experiments (NEX) = 2; 10 contiguous slices; resolution = 0.15 mm × 0.15 mm × 1.5 mm; acquisition time = 4 min). DWI (spin-echo EPIs, single-shot, 30 diffusion directions; TR/TE = 3000/46.398 ms; with b = 1000 s/mm^2 and 5 reference images (b = 0 s/mm^2); 10 contiguous slices, resolution = 0.3 mm × 0.3 mm × 1.5 mm with saturation slices at the edges of the field of view (FOV = 105 × 50, NEX = 2, acquisition time = 7 min). T2*-WI (FLASH 30 KHz, 10 slices; resolution = 0.12 mm × 0.10 mm × 1.5 mm; FOV = 256 × 256; TR/TE = 400/11 ms; NEX = 1; acquisition time = 1 m 42 s). MR angiography (FLASH 3D-time of flight (TOF) 32 slices; resolution = 0.13 mm × 0.18 mm × 0.17 mm;
FOV = 256 × 192; TR/TE = 10/2.09 ms; flip angle 20°; acquisition time = 1 m 21 s).

At the end of the last MRI acquisition, the rats were euthanized by a lethal concentration of isoflurane.

Image processing

The MRI images and reconstructed maps (for diffusion parameters) were analyzed in a masked manner using the image processing Paravision and in-house macros built on ImageJ software. Various indices were extracted from the DWI images: the eigenvectors (λ_1, λ_2, λ_3) and their measures, that is, the eigenvalues which were used to derive the mean ADC values defined by: $ADC = \frac{\lambda 1+\lambda 2+\lambda 3}{3}$, axial diffusivity $\lambda_1 = \lambda_{||}$, radial diffusivity $\lambda\perp$ defined by $\lambda\perp = \frac{\lambda 2+\lambda 3}{2}$ and FA defined by $FA = \frac{\sqrt{3\left(\left(\lambda 1-\sum\lambda\right)^2+\left(\lambda 2-\sum\lambda\right)^2+\left(\lambda 3-\sum\lambda\right)^2\right)}}{\sqrt{2(\lambda 1^2+\lambda 2^2+\lambda 3^2)}}$.[26]

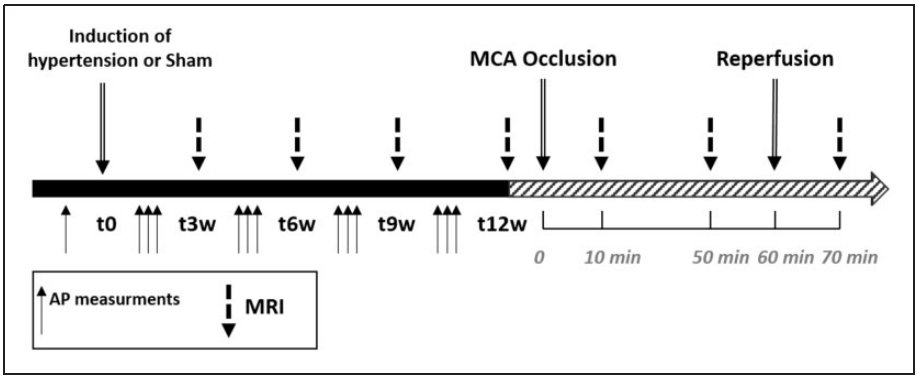

Figure 1. Experimental protocol: hypertension was induced at t0, and weekly measurements of systolic pressure (sAP) were made prior to magnetic resonance imaging (MRI). Twelve weeks after the induction of hypertension, the animals were subjected to transient (60 min) middle cerebral artery occlusion (MCAo).

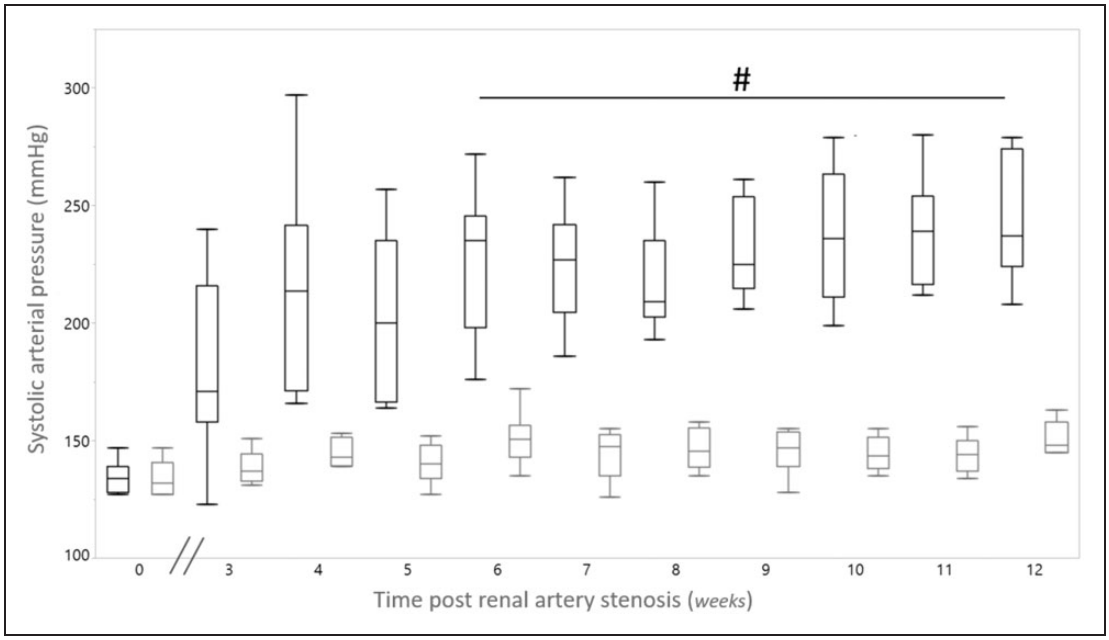

Figure 2. Evolution of systolic arterial pressure (sAP in mmHg) measured by the tail cuff method in hypertensive rats (HT) $n = 9$ ( ) and normotensive rats (NT) $n = 8$ ( ). The control period is represented by t0 and represents the measures performed before renal artery stenosis, $^{\#}p < 0.0001$ (two-way repeated measures ANOVA followed by Tukey's HSD test). The boxes define the interquartile range; the solid horizontal line represents the median, and the whiskers represent the minimal and maximal values.

Following the induction of ischemia, abnormal ADC values were automatically defined by thresholding the images at the mean minus 2 SD of the values of the contralateral (nonischemic) hemisphere after the exclusion of the ventricular volumes.[25] To quantify ADC, FA, $\lambda_{||}$, and $\lambda\perp$ in the cortex, the striatum, and the corpus callosum, regions of interest (ROIs) were manually delineated on four T2-WI coronal sections, over the antero-posterior brain axis, and then copied on coregistered DWI images. To estimate brain atrophy, both hemispheres (excluding the ventricles) were delineated on each T2-WI section, and their volumes calculated.

Statistical analyses

Data are represented as mean ± SEM. Statistical analyses were performed with analysis of variance (ANOVA) or two-way repeated measures ANOVA followed, where appropriate, by Tukey's honest significant difference (HSD) or by paired *t*-test with Bonferroni correction (JMP® software).

Results

Physiological parameters

In normotensive rats, mean sAP values remained stable during the study (135 ± 4 mmHg at the initiation and 138 ± 7 mmHg at the end) (Figure 2). However, in hypertensive animals, sAP increased progressively to reach a plateau 6 weeks following renal artery stenosis. There was an increase of 82% in sAP (134 ± 2 mmHg at the initiation and 244 ± 8 mmHg at the end) ($p < 0.0001$) (Figure 2). In the same animals, sAP was also significantly greater under anesthesia during the induction of ischemia and MRI acquisitions (Table 1). The other physiological parameters ($PaCO_2$, PaO_2, p_aH, and body temperature) were within the normal range and similar between the two groups of animals during both surgery and the MRI acquisitions (Table 1).

Spontaneous hypertension-induced neuropathological lesions prior to induced stroke

Evolution of T2-WI-derived signals. In normotensive rats no abnormal signal was observed irrespective of the time studied (Figure 3). None of the hypertensive animals displayed evident MRI abnormalities at 3 weeks following the induction of hypertension. However, from week 6 and thereafter, abnormal signals were apparent on T2-WI and were located in the grey matter in cortical and subcortical structures as well as in the bundles of white matter (Figure 3). The proportion of the animals that showed these abnormalities is the following: 4/9 at 6 weeks, 5/9 at 9 weeks, and 9/9 at 12 weeks. Some rats (6/9) developed progressively an enlargement of the cerebral ventricles (Figure 3). Petechial hemorrhages

Table 1. Physiological parameters.

	Before MCAo					Following MCAo					During MRI session				
	sAP	p_aH	p_aCO_2	p_aO_2	Temp.	sAP	p_aH	p_aCO_2	p_aO_2	Temp.	sAP	p_aH	p_aCO_2	p_aO_2	Temp.
NT	107 ± 5	7.43 ± 0.01	38.5 ± 1.0	125 ± 18	37.4 ± 0.2	138 ± 7	7.46 ± 0.02	36.3 ± 4	159 ± 20	37.8 ± 0.2	120 ± 7	7.39 ± 0.02	39.8 ± 3.2	138 ± 8	37.6 ± 0.1
HT	199 ± 12*	7.42 ± 0.01	40.6 ± 0.4	130 ± 17	37.6 ± 0.2	246 ± 8**	7.46 ± 0.02	40.9 ± 3.1	123 ± 15	37.9 ± 0.1	198 ± 5*	7.42 ± 0.02	40.8 ± 1.7	116 ± 7	37.6 ± 0.1

Note: All measurements were made under anesthesia. sAP: systolic arterial pressure in mmHg; Temp. = rectal temperature in °C; HT: hypertensive animals ($n = 9$); NT: normotensive animals ($n = 8$).
*$p < 0.05$, **$p < 0.01$ relative to normotensive animals (two-way repeated measures ANOVA followed by Tukey's HSD test).

occurred in grey matter and were evidenced on T2*-weighted MRI in 1/9 (6 weeks), 4/9 (9 weeks), and 6/9 (12 weeks) following the induction of hypertension (Figure 3) (see also online Supplementary Figure).

Despite these brain damages, hypertensive rats did not display any evident behavioral deficits during the experimental protocol.

Evolution of DWI–MRI-derived signals. We have quantified DWI-derived parameters (ADC, $\lambda_{||}$, $\lambda\perp$, and FA values) to address the question as to whether these parameters could be employed as biomarkers for CAH-induced brain lesions prior to the occurrence of stroke and could predict the extent of damage after the occurrence of stroke.

The analysis of ADC, in the corpus callosum, the motor cortex, the striatum as well as the whole hemisphere revealed time-related progressive reduction in normotensive rats (two-way ANOVA with repeated measures, time effect: $p < 0.001$, $p < 0.025$, $p < 0.038$, and $p < 0.02$, respectively, Figure 4(a)). However, while the hypertensive rats also displayed time-related changes in the striatum and in the corpus callosum (two-way ANOVA with repeated measures, time effect: $p < 0.014$ and $p < 0.021$ respectively, Figure 4(a)), they failed to show time related changes in the motor cortex as well as the entire hemisphere (two-way ANOVA with repeated measures, time effect: $p = 0.10$, $p = 0.15$, Figure 4(a)). When each time point was analyzed separately, the ADC values were significantly increased in hypertensive rats at 12 weeks after the induction of hypertension in the corpus callosum ($p < 0.05$), and a tendency toward an increase in the motor cortex was found ($p < 0.06$) (Figure 4(a)).

With respect to FA, there were time-related changes in normotensive animals (Figure 4(b)). In the corpus callosum, the FA increased over time (two-way ANOVA with repeated measures, time effect: $p < 0.05$, Figure 4(b)) and decreased in the cortex (two-way ANOVA with repeated measures, time effect: $p < 0.01$, Figure 4(b)). No changes were statistically significant in the hypertensive animals (two-way ANOVA with repeated measures, time effect: $p > 0.05$, Figure 4(b)) except for the motor cortex (two-way ANOVA with repeated measures, time effect: $p < 0.05$, Figure 4(b)). In the striatum, no time-related changes in hypertensive and normotensive rats were noted (two-way ANOVA with repeated measures, time effect: $p > 0.05$, Figure 4(b)). Although there was no global difference between the two groups when all the time points are concomitantly considered (two-way ANOVA with repeated measures, no group effect: $p > 0.35$, time effect $p < 0.05$ and no group × time interaction: $p > 0.5$), the comparison of the two groups at each time, taken separately, revealed that the FA decreased

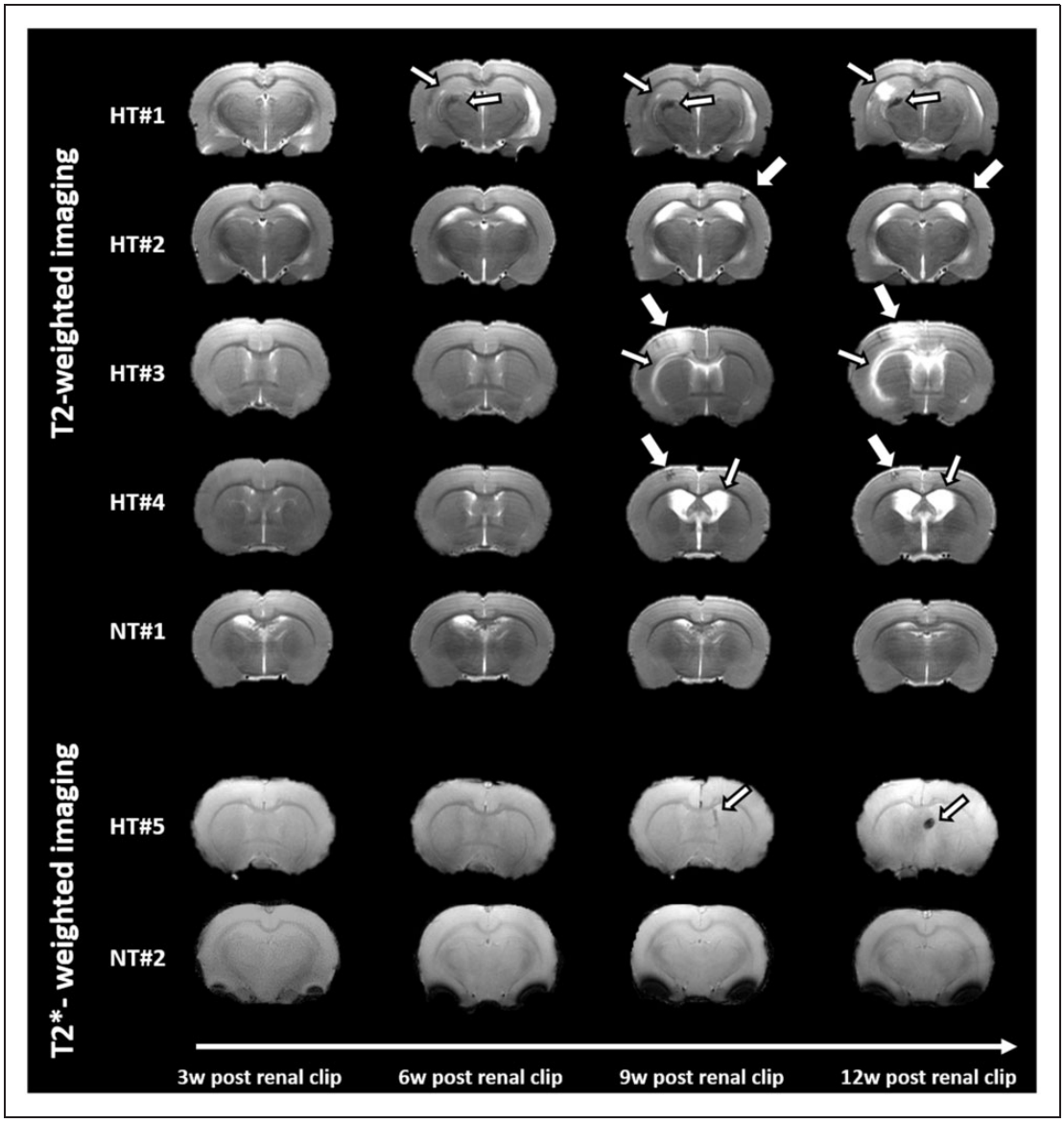

Figure 3. Hypertension-induced brain lesions. Lesions observed on T2-weighted imaging and T2*-weighted imaging in five hypertensive rats (HT) as a function of time. The abnormal signals are indicated by arrows. The normotensive (NT) rats failed to display any comparable observable signal.

in the corpus callosum of the hypertensive rats (t-test, $p < 0.05$) and increased in the cortex and the entire right hemisphere (t-test, $p < 0.05$) at 12 weeks following the induction of renovascular hypertension (Figure 4(b)).

When parallel and radial diffusions were quantified, no major and consistent differences were found between the hypertensive and normotensive rats (data not shown).

Hypertension-induced brain lesions following stroke

Evolution of MR angiography signal. Immediately after the MCAo, the animals were transferred to the MRI scanner and an MR angiography was performed. In all rats, irrespective of the group considered, the MCA disappeared which confirms the efficacy of the occlusion (Figure 5). There was no spontaneous reperfusion as witnessed by the persistence of the occlusion 50 min following the occlusion (Figure 5). The reperfusion instituted, 60 min following the occlusion, was successfully achieved in all rats as confirmed by the reappearance of the signal in the previously occluded MCA (Figure 5).

Evolution of diffusion abnormalities during and after MCAo. Ten minutes following the induction of ischemia, ADC maps revealed an exacerbated lesion in hypertensive compared to normotensive rats

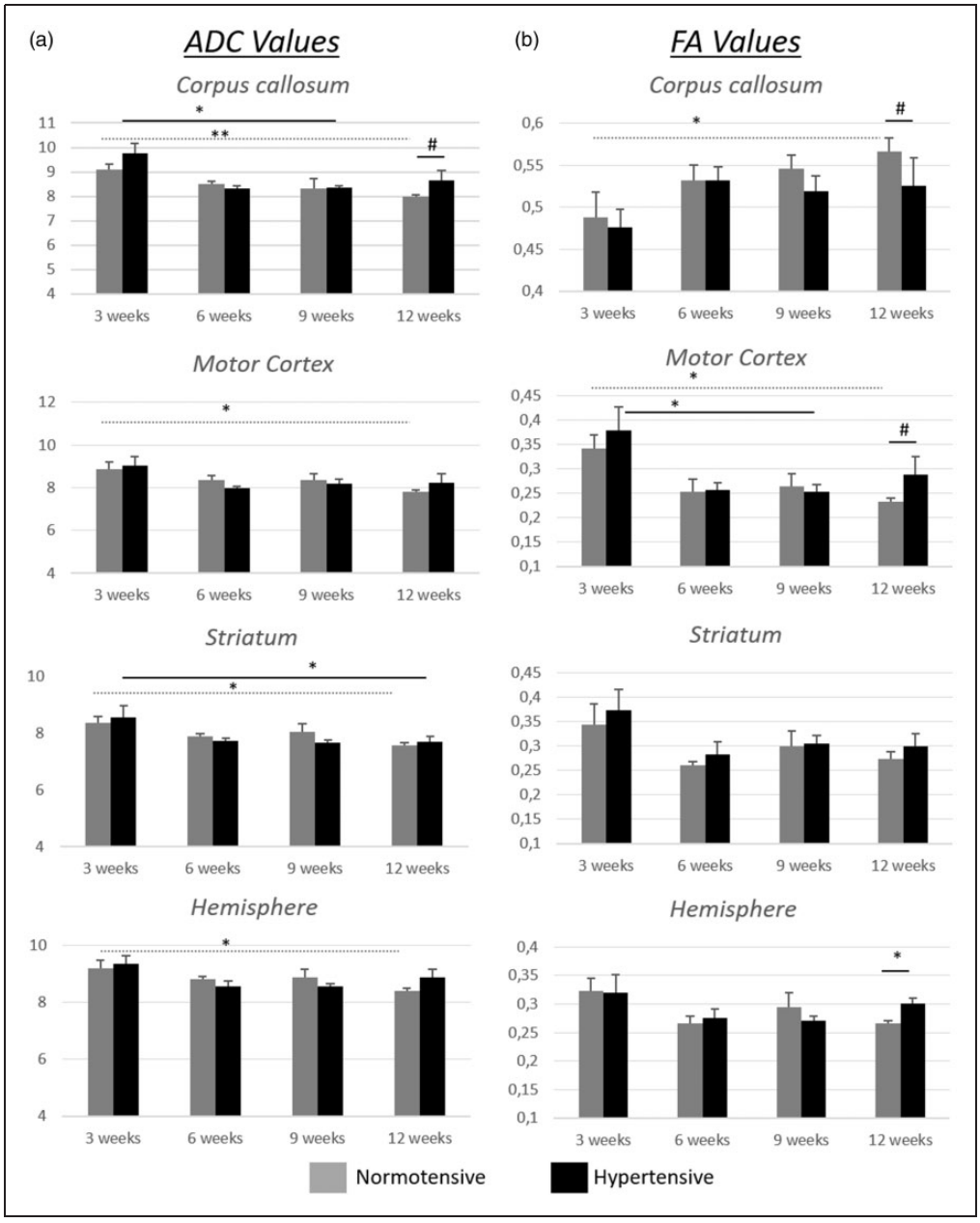

Figure 4. Evolution of apparent diffusion coefficient (ADC) (a) and fractional anistropy (FA) (b) values in the corpus callosum, striatum, motor cortex, and whole hemisphere during the rise of hypertension. $^{*}p < 0.05$, $^{**}p < 0.01$ (time effect, two-way repeated measures ANOVA), $^{\#}p < 0.05$ *t*-test.

($406 \pm 82\,mm^3$, $179 \pm 36\,mm^3$, respectively; $p < 0.02$) (Figure 6(a)). The difference in the volume of the lesion was maintained 50 min following the occlusion and 10 min following reperfusion ($452.1 \pm 70.8\,mm^3$ vs. $200.7 \pm 43.3\,mm^3$; $p < 0.02$ and $420.5 \pm 91.2\,mm^3$ vs. $142.9 \pm 30.9\,mm^3$; $p < 0.01$, respectively) (Figure 6(b)). Interestingly, in normotensive rats but not in hypertensive ones, reperfusion significantly decreased the volume of tissue that displayed ADC abnormalities ($p < 0.05$) (Figure 6(b)). Indeed, the threatened tissue salvaged by reperfusion was $20 \pm 9\%$ in the hypertensive rats and $41 \pm 8\%$ in the normotensive animals ($p < 0.05$) (Figure 6(c)).

Correlation between ADC before ischemia and lesion volume

The comparison between ADC values and the extent of the ischemic lesion revealed a significant correlation in hypertensive rats between the ADC values in the

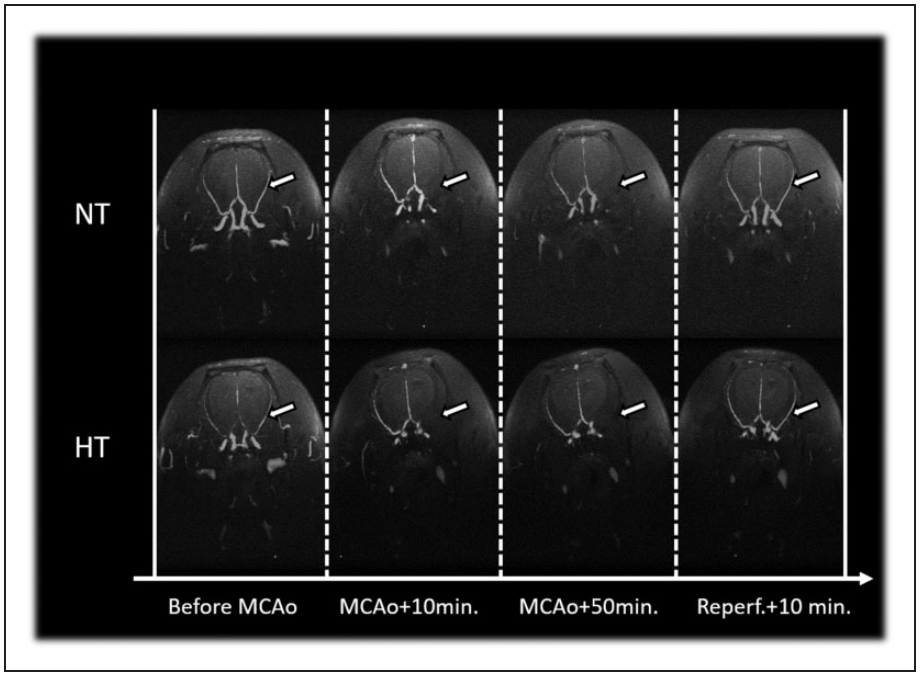

Figure 5. Representative MR angiography images before, and during MCAo (+10 min and +50 min) as well as at reperfusion in a normotensive rat (NT) and a hypertensive rat (HT). The white arrow points the right MCA. During MCAo, the hyperintense signal from the artery disappeared (MCA not distinguishable) and the right MCA signal reappeared immediately after reperfusion.

ipsilateral striatum 12 weeks after hypertension induction and the ADC defined lesion volume 50 min after ischemia ($R^2 = 0.47$, $p < 0.04$) (Figure 6(d)).

Discussion

It is established that hypertension is not only a major risk but also the most aggravating factor for ischemic stroke. Indeed, hypertension is responsible for more than 50% of patients presenting with an acute ischemic stroke. Despite these facts, CAH is rarely taken into account in preclinical studies of stroke.[27]

Although SHRs mimic many features of human essential hypertension, it is well established that the exacerbation of the ischemic lesion in this strain is not only due to the hypertension per se.[15] Accordingly, this issue is crucial to consider when SHRs are employed in stroke studies in which arterial hypertension is integrated. Therefore, an alternative and complementary model of hypertension should be employed.

In the present study, we have used a secondary hypertension model, namely the 2K-1C, in which hypertension is induced by a unilateral renal artery stenosis. The arterial blood pressure increased progressively and reached a plateau 6 weeks following the stenosis, which concords with the time-course previously reported.[25,28] With multiparametric MRI, we were able to analyze different structural variables during the development and the installation of hypertension.

These analyses revealed various alterations in brain tissue as soon as 6 weeks following the induction of hypertension. T2-weighted imaging revealed circumscribed lesions that affected the cortex, the striatum, the thalamus, and bundles of white matter (Figure 3). These spontaneous lesions increased in frequency and size as the time evolved to the extent such that all hypertensive animals displayed pathological signals at 12 weeks after the induction of hypertension. Those findings were consistent, in part, with a previous study conducted by Del Bigio et al.[17] in a more severe model of renovascular hypertension, namely the 2k-2C model. The authors reported that hypertensive rats displayed a rapid and severe increase in arterial pressure (sAP > 270 mmHg) that was accompanied by the formation of brain edema and infarction visible on T2-WI. Hypertension-induced brain lesions have also been reported in man.[29–33] These lesions could be attributed to the failure of cerebrovascular autoregulation and disturbed blood–brain barrier.[20,34]

We also noted profound hematomas and marked ventricular dilatation in the hypertensive rats, both pathologies are found in SHRs as well as in patients with hypertension.[35–37] The enlargement of the ventricles can be interpreted in two different ways: (1) the drainage of CSF is limited, which may result in an increase in intraventricular pressure with consequently ventricular dilatation, and/or (2) the loss of brain tissue is compensated by an enlargement of the ventricles.

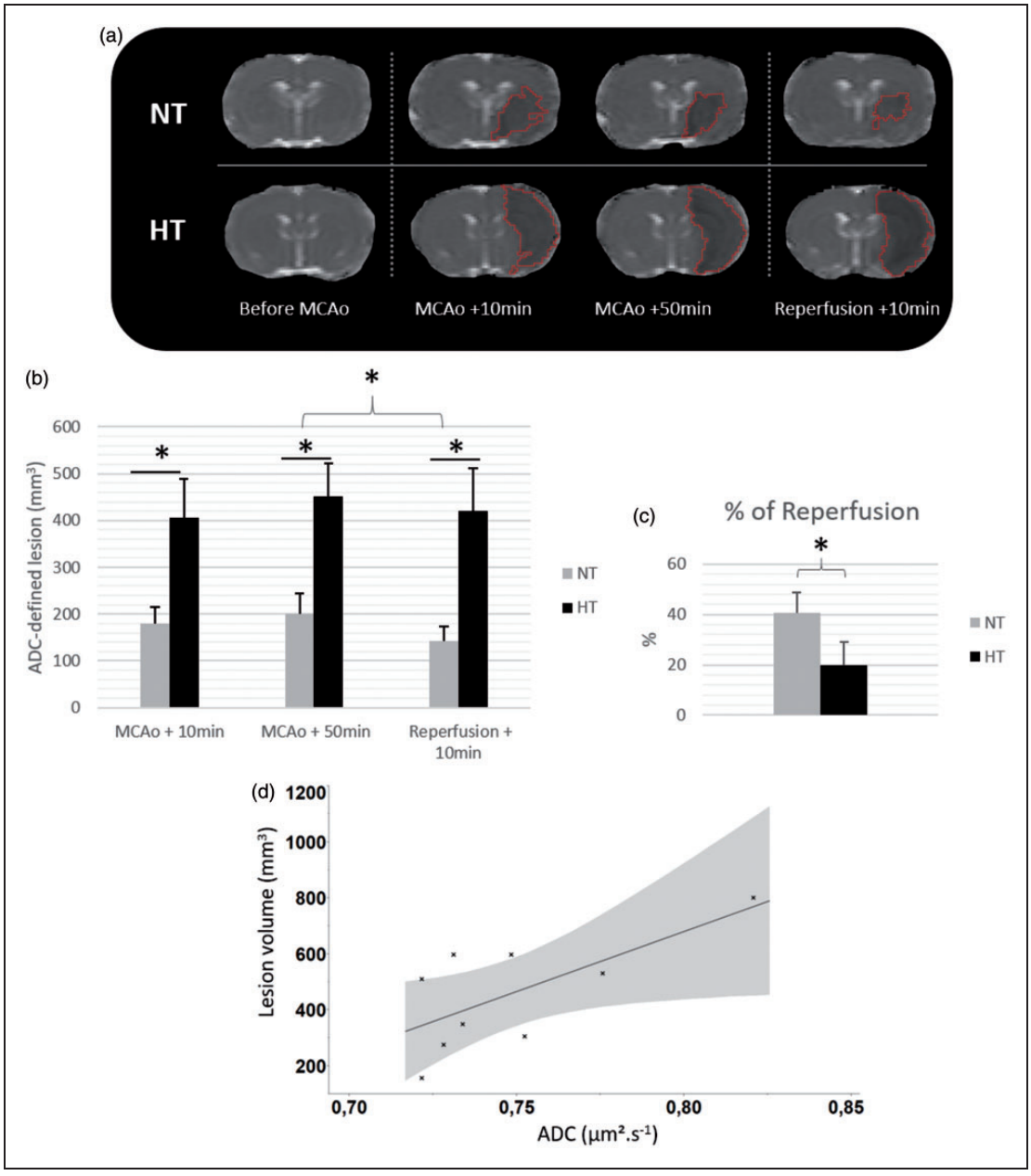

Figure 6. Representative ADC maps from normotensive (NT) and hypertensive (HT) rats before the occlusion and at 10 and 50 min postocclusion and 10 min post reperfusion (a). ADC-defined lesion volume in normotensive (NT) and hypertensive (HT) rats following the occlusion of the MCA and following reperfusion. *$p < 0.05$ (two-way repeated measures ANOVA followed by Tuckey HSD) (b). Percentage of tissue volume with abnormal ADC values salvaged by reperfusion. This volume is expressed as the volume of the lesion after reperfusion relative to that at 50 min postischemia. *$p < 0.05$ (*t*-test) (c). Correlation between striatal ADC values 12 weeks after the induction of hypertension and lesion volume at 50 min postischemia in hypertensive rats. $R^2 = 0.47$; $p < 0.04$ (linear regression) (d).

It seems that the latter hypothesis is the more plausible. SHRs, characterized by a ventricular enlargement, have normal intracranial pressure.[38,39] Taken together, cerebral atrophy could explain the dilatation of the ventricles as has been found in SHRs and hypertensive man.[40,41] In this latter study, it was suggested that hypertension induces an inevitable acceleration of brain atrophy, irreversible because even with anti-hypertensive therapy and controlled hypertension, those hypertensive subjects still showed a decline in brain matter.[41] In our study, hypertensive animals displayed a reduction of brain tissue volume (7%) compared to normotensive ones.

Overall the T2-WI data obtained in our studies strongly argue for the pertinence of the 2K-1C model to analyze the neuropathological signs of CAH. To extend these observations, we asked the question as to whether DWI–MRI could reveal more discrete

anomalies in the brain during the developmental and stable phases of hypertension, so as to provide noninvasive and early markers of the disease in hypertensive patients. DTI-derived parameters are increasingly documented to be a correlate of microstructural changes in different neurological diseases and therefore could provide noninvasive early markers of disease. In the context of CAH, identification of early cerebral changes associated with later development of stroke or dementia could be of importance in the management of hypertensive patients.

The quantification of the ADC values showed that normotensive animals exhibited a time-related decrease of this parameter in all the structures analyzed (Figure 4). This temporal decrease was not observed in hypertensive rats, especially when the whole hemisphere is considered, including both the cortex and the corpus callosum. An age-related decrease in ADC has been reported both in healthy animals and man.[42,43] It is postulated that the lower ADC values are correlated with the process of brain maturation. The maturation results in an increase in myelination and increased cell density and connectivity.[44] The different profiles of evolution of ADC observed in hypertensive animals would suggest that hypertension, to a certain degree, disturbs the normal organization of the brain. ADC modifications could be related to the relative increase in water content of the tissue as has been reported in SHR as well as in rats with renovascular hypertension.[17,24,34]

FA, which indicates the deviation from the isotropic diffusion of water molecules, was also altered in hypertensive animals in comparison to normotensive ones as was noted with the ADC data. This scalar parameter is an estimation of the cellular and tissular integrity and is increasingly employed in patients with neurological diseases such as stroke.[45] The FA was significantly decreased in the corpus callosum and increased in the cortex in hypertensive animals following 12 weeks of hypertension. These data, that are consistent with those reported by Lopez-Gil et al.[45] in SHR, and Wiesmann et al.[46] in mice in which hypertension was induced by angiotensin-II, again speak for hypertension-induced structural abnormalities in the brain. Such pathologies could underlie the cognitive deficits described in hypertensive subjects.[45,47] Although in our studies no overt behavioral defects were observed in hypertensive rats, even 12 weeks after the induction of hypertension where all the animals displayed discrete brain lesions, the use of adapted tests, be they cognitive, motor or sensory, could reveal impairments similar to those reported in SHR by Lopez-Gil et al.[45]

Our study also demonstrates that rats with chronic renovascular hypertensive suffer exacerbated brain infarcts as already described in the literature.[25] As early as 10 min after occlusion of the middle cerebral artery, the ADC-defined lesion in hypertensive animals was almost twice that of normotensive rats. Also worthy of note, although reperfusion significantly reversed the lesion in normotensive rats, it was less effective in hypertensive animals. These findings agree with our previous publication showing that the penumbra rapidly disappears in both SHRs and renovascular hypertensive rats.[25] Further support of this hypothesis is that thrombolysis with tissue-plasminogen activator t-PA is less effective in hypertensive animals and patients with uncontrolled hypertension.[48,49]

As the imaging paradigms employed in our studies are readily applicable to the clinical situation, our data argue for the importance of the analyses of DWI-derived parameters in patients presenting with uncontrolled CAH. Interestingly, we observed that ADC values within the striatum during established hypertension were correlated with the extent of ischemia-induced brain lesions. This correlation, that requires further corroboration, might suggest that ADC could be employed as a biomarker to predict the effects of hypertension on eventual stroke-induced lesions. Based on the above, it would be appropriate to analyze the effects of antihypertensive therapies on the evolution of these DWI-derived parameters.

Although our study has some limitations that may be improved (such as absence of quantification of cerebral blood flow changes and behavioral deficits during the development of hypertension and manual delimitations of some regions of interest), it permitted us to characterize a secondary hypertension model in which brain lesions occur during the chronic phase of hypertension reminiscent to those reported in hypertensive patients. This model also exhibits exacerbated ischemic brain lesions after MCA occlusion which make it a highly pertinent preclinical model which might be employed, alone or concomitantly with SHRs, in laboratory studies of the pathophysiology and the treatment of stroke.

Funding

The author(s) disclosed receipt of the following financial support for the research, authorship, and/or publication of this article: This work was supported by CNRS, the University of Caen Normandie, the TC2N Trans Channel Neuroscience Network Interreg IV A 2 Mers Seas Zeens program, Investing in your future crossborder cooperation program 2007–2014 part financed by the European Union (European Regional Development Fund), and the Conseil Régional de Basse-Normandie.

Declaration of conflicting interests

The author(s) declared no potential conflicts of interest with respect to the research, authorship, and/or publication of this article.

Authors' contributions

BM performed the experiments and data analyses, and drafted the manuscript. LC performed the hypertension model, SR supervised MRI studies and performed image analyses, MB revised the manuscript, OT designed the study, performed data analyses, and wrote the manuscript.

Supplementary material

Supplementary material for this paper can be found at the journal website: http://journals.sagepub.com/home/jcb

References

1. DiLuca M and Olesen J. The cost of brain diseases: a burden or a challenge? *Neuron* 2014; 82: 1205–1208.
2. Campbell BCV, Meretoja A, Donnan GA, et al. Twenty-year history of the evolution of stroke thrombolysis with intravenous alteplase to reduce long-term disability. *Stroke* 2015; 46: 2341–2346.
3. O'Collins VE, Macleod MR, Donnan GA, et al. 1,026 experimental treatments in acute stroke. *Ann Neurol* 2006; 59: 467–477.
4. Durukan A, Strbian D and Tatlisumak T. Rodent models of ischemic stroke: a useful tool for stroke drug development. *Curr Pharm Des* 2008; 14: 359–370.
5. Herson PS and Traystman RJ. Animal models of stroke: translational potential at present and in 2050. *Future Neurol* 2014; 9: 541–551.
6. Howells DW, Sena ES and Macleod MR. Bringing rigour to translational medicine. *Nat Rev Neurol* 2014; 10: 37–43.
7. Lawes CMM, Vander Hoorn S and Rodgers A. International Society of Hypertension. Global burden of blood-pressure-related disease. *Lancet* 2008; 371: 1513–1518.
8. Poulter NR, Prabhakaran D and Caulfield M. Hypertension. *Lancet* 2015; 386: 801–812.
9. O'Donnell MJ, Chin SL, Rangarajan S, et al. Global and regional effects of potentially modifiable risk factors associated with acute stroke in 32 countries (INTERSTROKE): a case–control study. *Lancet* 2016; 388: 761–775.
10. Fisher M, Feuerstein G, Howells DW, et al. Update of the stroke therapy academic industry roundtable preclinical recommendations. *Stroke* 2009; 40: 2244–2250.
11. Moskowitz MA, Grotta JC and Koroshetz WJ, Stroke Progress Review Group, National Institute of Neurological Disorders and Stroke. The NINDS Stroke Progress Review Group final analysis and recommendations. *Stroke* 2013; 44: 2343–2350.
12. Savitz SI, Cramer SC, Wechsler L, et al. Stem cells as an emerging paradigm in stroke 3: enhancing the development of clinical trials. *Stroke* 2014; 45: 634–639.
13. Duverger D and MacKenzie ET. The quantification of cerebral infarction following focal ischemia in the rat: influence of strain, arterial pressure, blood glucose concentration, and age. *J Cereb Blood Flow Metab* 1988; 8: 449–461.
14. Gratton JA, Sauter A, Rudin M, et al. Susceptibility to cerebral infarction in the stroke-prone spontaneously hypertensive rat is inherited as a dominant trait. *Stroke* 1998; 29: 690–694.
15. Lecrux C, Nicole O, Chazalviel L, et al. Spontaneously hypertensive rats are highly vulnerable to AMPA-induced brain lesions. *Stroke* 2007; 38: 3007–3015.
16. Fujishima M, Onoyama K, Oniki H, et al. Effects of acute hypertension on brain metabolism in normotensive, renovascular hypertensive and spontaneously hypertensive rats. *Stroke* 1978; 9: 349–353.
17. Del Bigio MR, Yan HJ, Kozlowski P, et al. Serial magnetic resonance imaging of rat brain after induction of renal hypertension. *Stroke* 1999; 30: 2440–2447.
18. Pullalarevu R, Akbar G and Teehan G. Secondary hypertension, issues in diagnosis and treatment. *Prim Care* 2014; 41: 749–764.
19. Weber BR and Dieter RS. Renal artery stenosis: epidemiology and treatment. *Int J Nephrol Renov Dis* 2014; 7: 169–181.
20. Wiesmann M, Kiliaan AJ and Claassen JA. Vascular aspects of cognitive impairment and dementia. *J Cereb Blood Flow Metab* 2013; 33: 1696–1706.
21. Barry DI, Strandgaard S, Graham DI, et al. Cerebral blood flow in rats with renal and spontaneous hypertension: resetting of the lower limit of autoregulation. *J Cereb Blood Flow Metab* 1982; 2: 347–353.
22. Stankevicius E, Martinez AC, Mulvany MJ, et al. Blunted acetylcholine relaxation and nitric oxide release in arteries from renal hypertensive rats. *J Hypertens* 2002; 20: 1571–1579.
23. Puig J, Blasco G, Schlaug G, et al. Diffusion tensor imaging as a prognostic biomarker for motor recovery and rehabilitation after stroke. *Neuroradiology* 2017 Mar 14. Epub ahead of print 14 March 2017. DOI: 10.1007/s00234-017-1816-0.
24. Sotak CH. The role of diffusion tensor imaging in the evaluation of ischemic brain injury – a review. *NMR Biomed* 2002; 15: 561–569.
25. Letourneur A, Roussel S, Toutain J, et al. Impact of genetic and renovascular chronic arterial hypertension on the acute spatiotemporal evolution of the ischemic penumbra: a sequential study with MRI in the rat. *J Cereb Blood Flow Metab* 2011; 31: 504–513.
26. Le Bihan D, Mangin JF, Poupon C, et al. Diffusion tensor imaging: concepts and applications. *J Magn Reson Imaging* 2001; 13: 534–546.
27. O'Collins VE, Donnan GA, Macleod MR, et al. Hypertension and experimental stroke therapies. *J Cereb Blood Flow Metab* 2013; 33: 1141–1147.
28. Oliveira-Sales EB, Toward MA, Campos RR, et al. Revealing the role of the autonomic nervous system in the development and maintenance of Goldblatt hypertension in rats. *Auton Neurosci Basic Clin* 2014; 183: 23–29.
29. Rosenberg EF. The brain in malignant hypertension: a clinicopathologic study. *Arch Intern Med* 1940; 65: 545–586.
30. Chester EM, Agamanolis DP, Banker BQ, et al. Hypertensive encephalopathy: a clinicopathologic study of 20 cases. *Neurology* 1978; 28: 928–939.

31. Fazekas F, Kleinert R, Offenbacher H, et al. Pathologic correlates of incidental MRI white matter signal hyperintensities. *Neurology* 1993; 43: 1683–1689.
32. Longstreth WT, Manolio TA, Arnold A, et al. Clinical correlates of white matter findings on cranial magnetic resonance imaging of 3301 elderly people. The Cardiovascular Health Study. *Stroke* 1996; 27: 1274–1282.
33. Verhaaren BF, Vernooij MW, de Boer R, et al. High blood pressure and cerebral white matter lesion progression in the general population. *Hypertension* 2013; 61: 1354–1359.
34. Mueller SM and Luft FC. The blood-brain barrier in renovascular hypertension. *Stroke* 1982; 13: 229–234.
35. Inatomi Y, Yonehara T, Hashimoto Y, et al. Correlation between ventricular enlargement and white matter changes. *J Neurol Sci* 2008; 269: 12–17.
36. Lee J-M, Zhai G, Liu Q, et al. Vascular permeability precedes spontaneous intracerebral hemorrhage in stroke-prone spontaneously hypertensive rats. *Stroke* 2007; 38: 3289–3291.
37. Sato S, Carcel C and Anderson CS. Blood pressure management after intracerebral hemorrhage. *Curr Treat Options Neurol* 2015; 17: 49.
38. Ritter S, Dinh TT, Stone S, et al. Cerebroventricular dilation in spontaneously hypertensive rats (SHRs) is not attenuated by reduction of blood pressure. *Brain Res* 1988; 450: 354–359.
39. Ritter S and Dinh TT. Progressive postnatal dilation of brain ventricles in spontaneously hypertensive rats. *Brain Res* 1986; 370: 327–332.
40. Kaiser D, Weise G, Möller K, et al. Spontaneous white matter damage, cognitive decline and neuroinflammation in middle-aged hypertensive rats: an animal model of early-stage cerebral small vessel disease. *Acta Neuropathol Commun* 2014; 2: 169.
41. Salerno JA, Murphy DG, Horwitz B, et al. Brain atrophy in hypertension. A volumetric magnetic resonance imaging study. *Hypertension* 1992; 20: 340–348.
42. Hagmann P, Sporns O, Madan N, et al. White matter maturation reshapes structural connectivity in the late developing human brain. *Proc Natl Acad Sci USA* 2010; 107: 19067–19072.
43. Heiland S, Sartor K, Martin E, et al. In vivo monitoring of age-related changes in rat brain using quantitative diffusion magnetic resonance imaging and magnetic resonance relaxometry. *Neurosci Lett* 2002; 334: 157–160.
44. Chabert S and Scifo P. Diffusion signal in magnetic resonance imaging: origin and interpretation in neurosciences. *Biol Res* 2007; 40: 385–400.
45. Lopez-Gil X, Amat-Roldan I, Tudela R, et al. DWI and complex brain network analysis predicts vascular cognitive impairment in spontaneous hypertensive rats undergoing executive function tests. *Front Aging Neurosci* 2014; 6: 167.
46. Wiesmann M, Roelofs M, van der Lugt R, et al. Angiotensin II, hypertension, and angiotensin II receptor antagonism: Roles in the behavioural and brain pathology of a mouse model of Alzheimer's disease. *J Cereb Blood Flow Metab*. Epub ahead of print 1 January 2016. DOI: 10.1177/0271678X16667364.
47. Obisesan TO. Hypertension and Cognitive Function. *Clin Geriatr Med* 2009; 25: 259–288.
48. Brinker G, Pillekamp F and Hossmann KA. Brain hemorrhages after rt-PA treatment of embolic stroke in spontaneously hypertensive rats. *Neuroreport* 1999; 10: 1943–1946.
49. Miller DJ, Simpson JR and Silver B. Safety of thrombolysis in acute ischemic stroke: a review of complications, risk factors, and newer technologies. *Neurohospitalist* 2011; 1: 138–147.